

A pair-based approximation for simplicial contagion

Federico Malizia,¹ Luca Gallo,² Mattia Frasca,³ Vito Latora,^{1,4,5,6} and Giovanni Russo⁷

¹*Department of Physics and Astronomy, University of Catania, 95125 Catania, Italy*

²*Department of Network and Data Science, Central European University, 1100 Vienna, Austria*

³*Department of Electrical, Electronics and Computer Science Engineering, University of Catania, 95125 Catania, Italy*

⁴*INFN Sezione di Catania, Via S. Sofia, 64, 95125 Catania, Italy*

⁵*School of Mathematical Sciences, Queen Mary University of London, London E1 4NS, UK*

⁶*Complexity Science Hub Vienna, A-1080 Vienna, Austria*

⁷*Department of Mathematics and Computer Science, University of Catania, 95125 Catania, Italy*

(Dated: July 20, 2023)

Pairwise interactions alone are often insufficient to characterize contagion processes, as more complex mechanisms involving groups of three or more individuals may be at play. Such higher-order interactions can be effectively modeled using frameworks beyond complex networks, such as simplicial complexes. The presence of these higher-order interactions has been shown to play a critical role in shaping the onset and evolution of contagion processes. However, studying these dynamics can be challenging due to the high dimensionality of the state space of these structures. To solve this problem, numerous mean-field models have been developed. Nevertheless, these models often overlook the correlations between different subsets of nodes, which can significantly influence the system dynamics. Therefore, more detailed approximations that account for these correlations are necessary. In this paper, we present a novel pair-based approximation for studying SIS dynamics on simplicial complexes. The pair-based approximation takes into consideration the dynamical correlations that emerge within groups of nodes in a simplicial complex. Compared to individual-based mean-field approaches, this approximation yields more accurate predictions of the behavior observed in stochastic simulations of contagion processes on simplicial complexes. Specifically, the proposed pair-based approximation provides higher accuracy in predicting the extent of the region of bistability, the type of the transition from a disease-free to an endemic state, and the average time evolution of the fraction of infected individuals. Overall, our findings highlight the significance of accounting for correlations within groups of nodes when investigating dynamical processes on simplicial complexes, and suggest that the pair-based approach can provide valuable insights into the behavior of such systems.

I. INTRODUCTION

Complex networks have been used to describe a large variety of dynamical processes involving interacting units, such as epidemic spreading [1, 2], social contagion [3], random walks [4], and synchronization [5], among many others. However, networks have inherent limitations as they can only capture interactions between pairs of units [6, 7]. Consequently, they cannot be employed to study complex systems characterized by interactions occurring in groups of three or more units [8]. In such cases, more sophisticated mathematical structures, such as hypergraphs [9] and simplicial complexes [10], are required. The inclusion of higher-order interactions has proved that these interactions give rise to novel collective phenomena in various dynamical processes [11], including diffusion [12, 13], synchronization [14–16], and evolutionary games [17].

In particular, the framework of higher-order networks has proven to be essential in modeling social contagion processes, such as opinion formation, rumor spreading, or the adoption of novelties, where the exposure to multiple sources is needed to trigger the transmission [18]. Recent studies of social contagion in hypergraphs [19] and simplicial complexes [20] have revealed that higher-order interactions may radically change the characteristics of the spreading process. In the presence of higher-order

interactions, the transition to an endemic state in SIS models can become discontinuous and a bistable regime where a disease-free and an endemic state co-exist can appear [19, 20]. This behavior is closely connected to the microscopic organization of higher-order interactions as diverse structures may exhibit different types of transitions [21].

Most models for the analysis of social contagion processes with higher-order interactions rely on individual-based mean-field approaches, assuming that the individuals are homogeneously mixed and interact with each other at random. However, this assumption may lead to an oversimplified approximation, as it overlooks the dynamic correlations that arise within the higher-order network. For example, infected individuals are more likely to come into contact with other infected individuals [2].

In the context of complex networks, to obtain a more precise description of the spreading process, one can consider more sophisticated approximations. For instance, pair-based models can be employed [22–25]. In these models, the system dynamics is not characterized at the level of nodes, that is, it does not follow the temporal evolution of the expected number of individuals in a given state, but it is described at the level of pairs of nodes, namely it analyzes how the expected number of edges in a given state evolves in time.

However, deriving mean-field models for spreading pro-

cesses on structures with higher-order interactions is more challenging, resulting in a smaller number of available approaches. In this work, we consider the same contagion process studied in [20], namely an SIS process in the presence of three-body simplicial interactions, and develop a mean-field model based on a description at the level of the pairs, which we then analyse in comparison with the individual-based mean-field model introduced in [20].

In the past years, a few works have investigated the development of mean-field models for contagion dynamics in the presence of higher-order interactions [26, 27]. In particular, in [26] a model relying on a discrete-time Markov-chain approach has been proposed. In this model, the system dynamics is expressed in terms of joint probabilities of the microscopic states of the links and the nodes, and thus is described by a set of $N + L$ master equations, where N is the number of nodes and L the number of links. In our work, instead, we consider a continuous-time framework yielding a system of governing equations whose order does not depend on the number of nodes and links. The model developed in [27] also adopts a continuous-time framework, but relies on the assumption that adjacent hyperedges share at most one node. In our work, instead, we tackle the more general case that includes all possible motifs of three and four nodes that can exist in a simplicial complex.

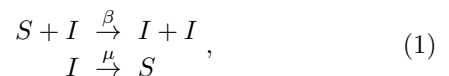
The rest of the paper is organized as follows. In Sec. II we provide some preliminary results, recalling the individual-based and the pair-based approximation of the SIS model on networks, and then describing the individual-based approximation for the SIS model on simplicial complexes. In Sec. III we introduce the pair-based approximation of the simplicial SIS model and its derivation. In Sec. IV, we compare the predictions of the individual-based and the pair-based approximation for the simplicial SIS model. Finally, in Sec. V we summarize and discuss the main results obtained.

II. MEAN-FIELD SIS MODELS

In this section, we first discuss two different mean-field approximations for the SIS model on networks, namely a contagion process where the disease can be transmitted exclusively occurs through pairwise interactions. We describe both the individual-based and pair-based approximations, highlighting the fundamental mechanisms involved in deriving mean-field models at the individual- and pair-based levels. Subsequently, we revisit the individual-based approximation for the simplicial SIS model studied in [20]. This will lay the groundwork for introducing the pair-based approximation for the simplicial SIS model in Sec. III.

A. Individual-based mean-field SIS model

We begin by characterizing the processes governing the transition of an individual from one state to another in the standard SIS model. In this model, an individual can be either susceptible (S) or infected/infectious (I), and can transit from one compartment to another as infection or recovery takes place. In the former process, a susceptible individual (S) becomes infected (S→I) after interacting with an infectious individual (I), which acts a mediator of the transition. Hence, the infection mechanism is a two-body nonlinear process. In the second case, an infected individual (I) recovers after a given period of time, becoming once again susceptible (I→S). At variance with the infection mechanism, the recovery is described by a one-body linear process. Formally, we can express these transitions in terms of two kinetic equations



where β and μ represent the transition rates for the infection and the recovery process, respectively.

The dynamics of the SIS model on a network can be investigated using different approaches [1, 2]. A commonly employed strategy is to perform stochastic simulations of the kinetic equations (1). However, this approach has some limitations. Firstly, it can be computationally expensive for large networks. Additionally, it requires a significant amount of data, as both the contact network and the states of the nodes need to be known empirically. Moreover, this approach does not facilitate understanding of the relationship between the model parameters and the emerging collective behavior [25]. For this reason, a common approach is to make use of a deterministic representation of the process that focuses on population-level quantities, such as the density or the expected number of individuals in a given state. This deterministic approach assumes homogeneous mixing, where the interactions between individuals are treated as uniform and independent of the network structure, so that each individual can be considered statistically equivalent to any other. This hypothesis allows to describe the dynamics of the system in terms of a so-called mean-field model.

For the SIS model under homogeneous mixing, the dynamics is described by the following equations

$$\begin{aligned} \dot{\langle S \rangle} &= \mu \langle I \rangle - \beta k \langle SI \rangle \\ \dot{\langle I \rangle} &= -\mu \langle I \rangle + \beta k \langle SI \rangle \end{aligned}, \quad (2)$$

where $\langle S \rangle$ and $\langle I \rangle$ represent the densities of susceptible and infected individuals, respectively, $\langle SI \rangle$ is the density of edges in the state (S, I) , i.e., a susceptible individual in contact with an infectious one, while k is the average node degree. The densities of individuals in state S and I are given by $\langle S \rangle = [S] / N$ and $\langle I \rangle = [I] / N$, where $[S]$ and $[I]$ are the expected number of susceptible and infected individuals, respectively, and $N = [S] + [I]$ is the total

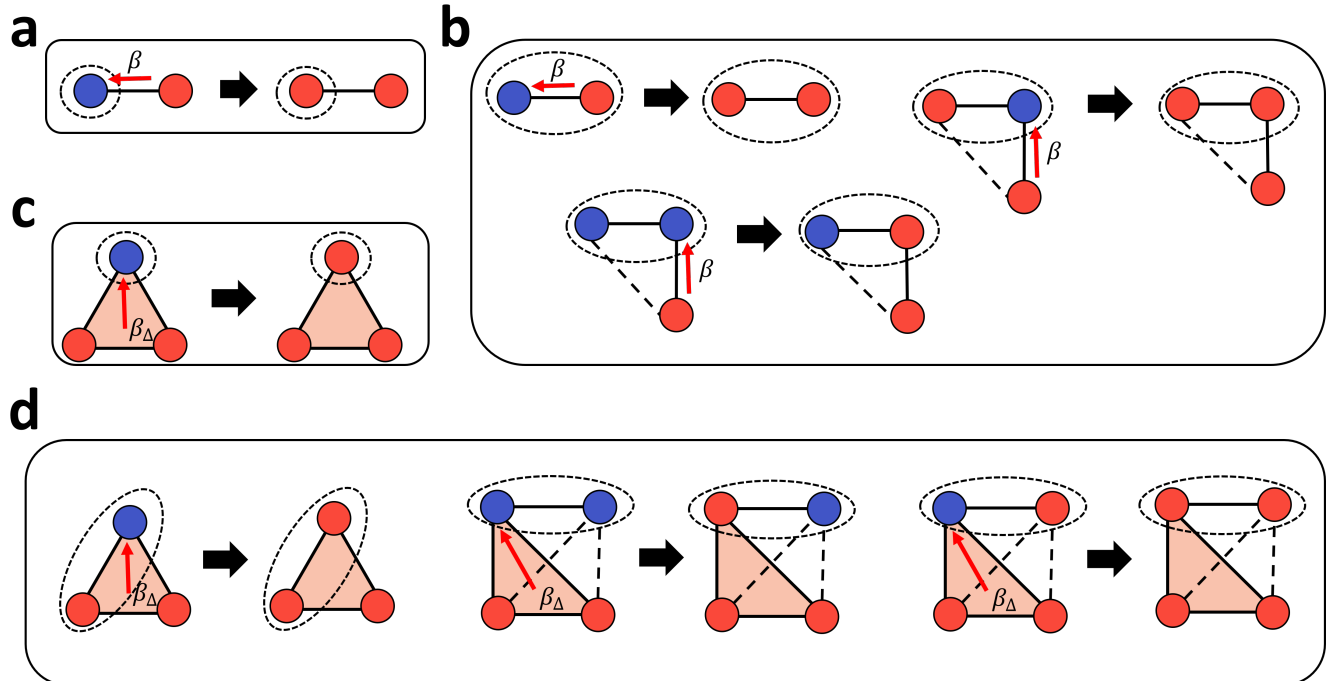


FIG. 1. Pictorial representation of infection processes among susceptible (in blue) and infected (in red) individuals in SIS models. (a) Infection of a node connected to an infected node through a link. This is the only infection process occurring in the individual-based SIS model. (b) Infection in a pair of nodes. In a pair-based description of contagion in a SIS model, the disease can be transmitted to one of the nodes of a pair by the other node of the pair or by other infected nodes, not belonging to the pair. (c) Simplicial infection in a triangle by group interaction with two infected nodes. This infection process characterizes contagion in simplicial SIS models. (d) Infection in a pair of nodes in the presence of group interactions. The infection processes depicted in panel (d) arise in the pair-based description of the simplicial SIS model.

number of individuals in the population. Consequently, $\langle S \rangle$ and $\langle I \rangle$ are related through the conservation relation $\langle S \rangle + \langle I \rangle = 1$, so they are not independent. The density $\langle SI \rangle$ is defined as $\langle SI \rangle = [SI] / kN$, where $[SI]$ represents the expected number of edges in state (S, I) . Note that $kN = 2L$, where L is the total number of edges within the network. The two terms in the equation for $\langle I \rangle$ represent the decrease in the density of infectious individuals due to recoveries, and the increase in the same density due to infections, respectively. The first depends on the transition rate μ and on the density of infected individuals, while the second is given by the product of the transition rate β by the average degree k and the edge density $\langle SI \rangle$. The transition from susceptible to infected through the interaction with an infected individual is depicted in panel (a) of Fig. 1.

System (2) is exact but not closed, as the equations governing the dynamics of both $\langle S \rangle$ and $\langle I \rangle$ depend on the quantity $\langle SI \rangle$. To obtain a closed system of equations, one may apply the law of mass action, which consists of assuming statistical independence at the level of individuals. This means to assume that infected individuals are randomly distributed in the network, so that the probability that a neighbor is infected is given by $\langle I \rangle$ and does not depend on the state of the node itself. Under

this assumption, by approximating the fraction of edges in state (S, I) as

$$\langle SI \rangle \approx \langle S \rangle \langle I \rangle, \quad (3)$$

and substituting this expression in Eqs. (2), we obtain the following closed form for the mean-field SIS model:

$$\begin{aligned} \dot{\langle S \rangle} &= \mu \langle I \rangle - \beta k \langle S \rangle \langle I \rangle \\ \dot{\langle I \rangle} &= -\mu \langle I \rangle + \beta k \langle S \rangle \langle I \rangle \end{aligned} \quad (4)$$

B. Pair-based mean-field SIS model

Assuming that infected individuals are randomly distributed in the network may lead to an oversimplified approximation, as it does not account for the dynamic correlations that exist within the contact network (for example, infected nodes are more likely to come into contact with other infected nodes) [1]. To provide a more accurate description of the SIS dynamics on a network, one can consider a pair-based model, which incorporates these dynamic correlations. In practice, one has to characterize the system dynamics at the level of pairs of nodes, describing how the expected number of edges in

a given state evolves in time. For the SIS process, the equations describing the SIS process at the pair-level are:

$$\begin{aligned} \langle \dot{S} \rangle &= \mu \langle I \rangle - \beta k \langle SI \rangle \\ \langle \dot{I} \rangle &= -\mu \langle I \rangle + \beta k \langle SI \rangle \\ \langle \dot{SS} \rangle &= 2\mu \langle SI \rangle - 2\beta(k-1) \langle SSI \rangle \\ \langle \dot{SI} \rangle &= \mu \langle II \rangle - \mu \langle SI \rangle + \beta(k-1) \langle SSI \rangle \\ &\quad - \beta(k-1) \langle ISI \rangle - \beta \langle SI \rangle \\ \langle \dot{II} \rangle &= -2\mu \langle II \rangle + 2\beta(k-1) \langle ISI \rangle + 2\beta \langle SI \rangle \end{aligned} \quad (5)$$

where $\langle ISI \rangle$ represents the density of (open and closed) triplets in state (I, S, I) , and is defined as $\langle ISI \rangle = [ISI] / (k(k-1)N)$, with $[ISI]$ being the expected number of triplets in that state. Note that the term $k(k-1)$ corresponds to the average number of triplets connected to each node. Indeed, each node i with k neighbors is at the center of $k(k-1)/2$ unordered triples. $\langle S \rangle$ and $\langle I \rangle$ can be obtained from $\langle SS \rangle$, $\langle SI \rangle$ and $\langle II \rangle$ through marginalization, namely $\langle S \rangle = \langle SS \rangle + \langle SI \rangle$ and $\langle I \rangle = \langle SI \rangle + \langle II \rangle$. Additionally, $\langle SS \rangle$, $\langle SI \rangle$ and $\langle II \rangle$ are not independent, as they are linked through the conservation relation $\langle SS \rangle + 2\langle SI \rangle + \langle II \rangle = 1$. Note that, with respect to the individual-based approximation, the pair-based SIS model contains a higher number of terms, reflecting the higher number of possible states and transitions that a pair has compared to a single node.

To illustrate the terms appearing in Eqs. (5), let us focus on the equation governing the dynamics of $\langle SI \rangle$. The first two terms are related to recoveries. Indeed, the first term represents the increase in the density $\langle SI \rangle$ due to the recovery of one of the nodes of the pairs in state (I, I) . The second term models the decrease in $\langle SI \rangle$ due to the recovery of the infected nodes of the pairs in state (S, I) , i.e., the transition from (S, I) to (S, S) . The remaining three terms encode the possible transitions of an edge due to infections, as graphically represented in panel (b) of Fig. 1. In particular, the first encodes the increase in $\langle SI \rangle$ due to the infection of one of the nodes in the pairs in (S, S) , while the second represents the decrease in $\langle SI \rangle$ due to the infection of the susceptible nodes in the pairs in state (S, I) . Both transitions are due to the interaction with a third (infectious) node, among the $(k-1)$ remaining neighbors of the susceptible nodes. Note that the three nodes involved in the interaction can be arranged in two possible motifs, namely an open triangle, i.e., a wedge, or a closed one. This point will turn out to be crucial when considering the closure of the system. The last term corresponds to the decrease in $\langle SI \rangle$ due to the infection of the susceptible nodes in the pairs in state (S, I) . In this case, however, the transition is due to the infected nodes of the pair, and not to a third node.

System (5) is exact but not closed. Different approximations of the triplet densities have been proposed to close the system at the pair level. The most common and studied one [1] consists of writing the probability that a motif is in a given state as the product of the probabilities that its edges are in a certain state, normalized by

the probabilities that the nodes in common to the pairs of edges are in a particular state. To illustrate it, let us first consider a triple of nodes i , j , and z , in states A, B, and C respectively, forming a wedge, so that node j is connected to nodes i and z , while i and z are not linked. We can write the density of wedges in state (A, B, C) as

$$\langle ABC^\wedge \rangle \approx \frac{\langle AB \rangle \langle BC \rangle}{\langle B \rangle}, \quad (6)$$

where $\langle AB \rangle = P(AB)$ and $\langle BC \rangle = P(BC)$ are the probabilities that links (i, j) and (j, k) are in states (A, B) and (B, C) , respectively, while $\langle B \rangle$ is the probability that node j is in state B. This formula can be obtained as follows.

$$\langle ABC^\wedge \rangle = P(AB \cap BC) = P(BC)P(AB|BC)$$

where $P(AN|BC)$ denotes the conditional probability that i and j are in states A and B, given that j and z are in states B and C. Then we make the approximation

$$P(AB|BC) \approx P(AB|B) = P(AB)/P(B)$$

Combining these two relations we obtain Eq. (6). When there are few short cycles, i.e., few closed triangles, in the network, Eq. (6) represents an accurate approximation of the probability that a triplet of nodes is in state (A, B, C) . However, this closure fails to describe the epidemic dynamics on networks where the number of closed triplets is not negligible [1, 22], as it overlooks the correlation between nodes i and k . Therefore, in the case of a triple of nodes i , j , and z forming a closed triangle, one usually approximates the density of triangles in state (A, B, C) using the so-called Kirkwood superposition [28], namely [29]

$$\langle ABC^\Delta \rangle \approx \frac{\langle AB \rangle \langle BC \rangle \langle AC \rangle}{\langle A \rangle \langle B \rangle \langle C \rangle}. \quad (7)$$

Note that, when we assume the dynamics of nodes i and z to be uncorrelated, i.e., $\langle AC \rangle = \langle A \rangle \langle C \rangle$, we find that the approximation for $\langle ABC^\Delta \rangle$ recovers the one for $\langle ABC^\wedge \rangle$.

The next step is to calculate the probability that a generic triplet of nodes is in state (A, B, C) , namely $\langle ABC \rangle$, as a function of $\langle ABC^\wedge \rangle$ and $\langle ABC^\Delta \rangle$. To this aim, let us consider the global clustering coefficient $\phi \in [0, 1]$, representing the fraction of closed triangles over all triplets in the structure, and calculate it in a statistical meaning as

$$\phi = \frac{3\mathbb{E}(\mathcal{T})}{Nk(k-1)}, \quad (8)$$

where N is the number of nodes, k is the average number of links (i.e., 1-simplices) per node, and $\mathbb{E}(\mathcal{T})$ represents the expected number of triangles, which depends on the structure considered. At this point, we can calculate

$\langle ABC \rangle$ as [1, 22]:

$$\langle ABC \rangle = (1 - \phi)\langle ABC^\wedge \rangle + \phi\langle ABC^\Delta \rangle. \quad (9)$$

Note that the densities $\langle ABC^\wedge \rangle$ and $\langle ABC^\Delta \rangle$ are defined as $\langle ABC^\wedge \rangle = [ABC^\wedge]/k(k-1)(1-\phi)N$ and $\langle ABC^\Delta \rangle = [ABC^\Delta]/k(k-1)\phi N$, where $[ABC^\wedge]$ $[ABC^\Delta]$ are the expected number of wedges and of triangles in state (A, B, C) respectively.

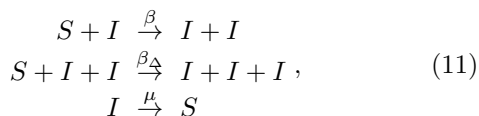
Hereafter, we will consider Eq. (9) to close the compartmental models at the pair level. In particular, we will approximate the densities $\langle SSI \rangle$ and $\langle ISI \rangle$ as:

$$\begin{aligned} \langle SSI \rangle &\approx (1 - \phi) \frac{\langle SS \rangle \langle SI \rangle}{\langle S \rangle} + \phi \frac{\langle SS \rangle \langle SI \rangle^2}{\langle S \rangle^2 \langle I \rangle} \\ \langle ISI \rangle &\approx (1 - \phi) \frac{\langle SI \rangle^2}{\langle S \rangle} + \phi \frac{\langle SI \rangle^2 \langle II \rangle}{\langle S \rangle \langle I \rangle^2}. \end{aligned} \quad (10)$$

Such closure relations are a direct consequence of Eqs. (6)-(9). Eqs. (5) along with the expressions (10) constitute a closed approximation for the pair-based mean-field SIS model.

C. Individual-based mean-field simplicial SIS model

We now discuss the individual-based mean-field simplicial SIS model, presented in [20]. As done for the SIS model on networks, i.e., in the absence of higher-order interactions, we first describe the processes ruling the transition of an individual from one state to another, this time in the presence of high-order interactions. In this case, in addition to the infection processes occurring in the SIS model on networks, there is a further way in which an individual transits from one compartment to another. In fact, a susceptible individual (S) can become infected (S \rightarrow I) through a three-body interaction, in which the other two individuals are infectious. In this case, both infected individuals act as mediators of the transition. Similarly to the network case, we can represent the processes of the simplicial SIS model in terms of kinetic equations



where β and β_Δ are the transition rates for the two-body and the three-body infection process, respectively, while μ is the recovery rate.

We now derive a model that describes the system dynamics in terms of population-level quantities. Under the homogeneous mixing hypothesis, the exact equations for the simplicial SIS model are given by

$$\begin{aligned} \dot{\langle S \rangle} &= \mu \langle I \rangle - \beta k \langle SI \rangle - \beta_\Delta k(k-1)\phi\delta \langle ISI^\Delta \rangle \\ \dot{\langle I \rangle} &= -\mu \langle I \rangle + \beta k \langle SI \rangle + \beta_\Delta k(k-1)\phi\delta \langle ISI^\Delta \rangle, \end{aligned} \quad (12)$$

where $\delta \in [0, 1]$ is the fraction of triangles that are effectively 2-simplices. Compared to Eqs. (2), these equations present an additional term, i.e., $\beta_\Delta k(k-1)\phi\delta \langle ISI^\Delta \rangle$, which takes into account the contribution of the three-body interactions, namely the infection of a susceptible node due to the simultaneous interaction with two infected individuals, as shown in panel (c) of Fig. 1.

System (12) may be closed by applying the law of mass action, starting from the assumption that infected individuals are randomly distributed in the simplicial complex [20]. Accordingly, the density $\langle ISI^\Delta \rangle$ is approximated as

$$\langle ISI^\Delta \rangle \approx \langle I \rangle \langle S \rangle \langle I \rangle, \quad (13)$$

which allows us to write the individual-based mean-field model for the simplicial SIS model as follows:

$$\begin{aligned} \dot{\langle S \rangle} &= \mu \langle I \rangle - \beta k \langle S \rangle \langle I \rangle - \beta_\Delta k_\Delta \langle S \rangle \langle I \rangle^2 \\ \dot{\langle I \rangle} &= -\mu \langle I \rangle + \beta k \langle S \rangle \langle I \rangle + \beta_\Delta k_\Delta \langle S \rangle \langle I \rangle^2, \end{aligned} \quad (14)$$

where $k_\Delta = k(k-1)\phi\delta$ represents the average number of 2-simplices connected to each node.

The system can be analytically investigated in terms of two parameters, $\lambda = k\beta/\mu$ and $\lambda_\Delta = k_\Delta\beta_\Delta/\mu$, representing respectively the rescaled infectivity on 1-simplices and on 2-simplices. In particular, this permits to obtain the steady-state solutions of Eqs. (14) and to study their stability as a function of λ and λ_Δ . The analysis shows that, when the higher-order interactions are weak, i.e., when $\lambda_\Delta < 1$, the system behaves similarly to the SIS model on networks, described by Eq. (2): for $\lambda < 1$ the disease-free equilibrium $\langle I \rangle^* = 0$ is the only solution, while for $\lambda > 1$ a stable endemic state $\langle I \rangle^* \neq 0$ exists. In addition, the phase transition at $\lambda = 1$ is continuous. However, when the higher-order interactions are stronger, i.e., $\lambda_\Delta > 1$, the system shows a different behavior. For λ smaller than $\lambda_c = 2\sqrt{\lambda_\Delta} - \lambda_\Delta$, only the disease-free equilibrium exists. For $\lambda_c < \lambda < 1$, the disease-free equilibrium and an endemic state coexist in a bistable regime, with the initial fraction of infected individuals determining whether the system reaches one equilibrium point or the other: if the initial fraction of infected individuals is larger than a critical mass, then the system evolves towards the endemic state; otherwise the disease spreading cannot be sustained, and the system evolves towards the disease-free equilibrium. Finally, for $\lambda > 1$, the endemic state is the only stable equilibrium. Differently from the SIS model on networks, when $\lambda_\Delta > 1$ the phase transition occurring at $\lambda = \lambda_c$ and $\lambda = 1$ is discontinuous.

III. A PAIR-BASED APPROXIMATION FOR THE SIMPLICIAL SIS MODEL

In this section, we derive the pair-based mean-field simplicial SIS model. To this aim, we have to account

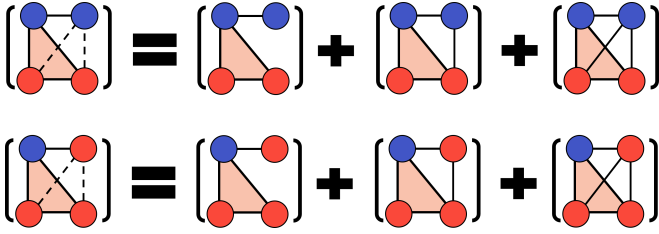


FIG. 2. Graphical representation of the three possible microscopical configurations of four-node motif states (I, I, S, S) (on top) and (I, I, S, I) (bottom). Square brackets refer to the expected number of the singular configurations.

for all ways a pair of nodes in a simplicial complex can transit from one state to another. Besides the ones already discussed in the derivation of the previous models, the transitions illustrated in panel (d) of Fig. 1 should also be considered. Remarkably, two of these transitions depend on the state of 4-node motifs, and occur when the 2-simplex shares with the edge of interest a single node. Instead, the remaining one depends of the state of a 3-node motif, and corresponds to the case where the focal edge belongs to the 2-simplex. In the first two cases, an infection can occur when the shared node is susceptible and the other nodes of the 2-simplex are infected, while the other node in the pair can be either susceptible or infected. Hence, both the densities of edges in states (S, S) and (S, I) are affected by this infection process, with a rate that is function of the rate β_Δ and of the density of 4-node motifs in the aforementioned states. As shown in Fig. 2, there are three possible motifs that contribute to this infection process. They differ for the number of links (zero, one or two) that connect the node external to the 2-simplex to the infected nodes of the 2-simplex. Hereby, we denote as $\langle IIS^\Delta S \rangle_0$, $\langle IIS^\Delta S \rangle_1$, and $\langle IIS^\Delta S \rangle_2$ the densities of these motifs in state (I, I, S, S) , while we denote as $\langle IIS^\Delta I \rangle_0$, $\langle IIS^\Delta I \rangle_1$, and $\langle IIS^\Delta I \rangle_2$ the density of motifs in state (I, I, S, I) . More in general, using the clustering coefficient ϕ , we can write the density of 4-node motifs in states (I, I, S, S) and (I, I, S, I) as

$$\begin{aligned}
 \langle IIS^\Delta S \rangle &= (1 - \phi)^2 \langle IIS^\Delta S \rangle_0 \\
 &\quad + 2(1 - \phi)\phi \langle IIS^\Delta S \rangle_1 \\
 &\quad + \phi^2 \langle IIS^\Delta S \rangle_2 \\
 \langle IIS^\Delta I \rangle &= (1 - \phi)^2 \langle IIS^\Delta I \rangle_0 \\
 &\quad + (1 - \phi)\phi \langle IIS^\Delta I \rangle_1 \\
 &\quad + \phi^2 \langle IIS^\Delta I \rangle_2
 \end{aligned} \tag{15}$$

In order to quantify the contribution to the model equations of the two transitions involving the state of 4-node motifs, we also need to calculate the average number of motifs in which the pair of nodes is not part of the 2-simplex. As each node is connected to k links on average, the average number of motifs composed by a 2-simplex connected to a link is $k(k-1)\phi\delta(k-2)$. Indeed, the average number of 2-simplices connected to a node

is $k(k-1)\phi\delta$, while the fourth node of the motif has to be chosen among the $(k-2)$ remaining neighbors of the node.

Let us now go back to the infection process that is shown in panel (d) of Fig. 1 and involves the 3-node motifs. In this case, the node pair is part of the 2-simplex. Here, the only possible transition for the edge is the one from state (S, I) to state (I, I) . In fact, both the two other nodes of the 2-simplex have to be in the infectious state to yield a simplicial contagion, as expressed by the second kinetic equation (11). Similarly to the previous case, the overall contribution present in the model will depend on the infection rate β_Δ , on the density of 2-simplices in state (I, I, S) , which we denote as $\langle IIS^\Delta \rangle$, and on the average number of triangles an edge is part of. In particular, the latter is given by $2(k-1)\phi\delta = 2k_\Delta/k$, where the factor 2 comes from the fact that each 2-simplex has two edges pointing to a node.

Taking into account the previous considerations, we can finally write the equations governing the simplicial SIS model at the pair-level:

$$\begin{aligned}
 \langle \dot{S} \rangle &= \mu \langle I \rangle - \beta k \langle SI \rangle - \beta_\Delta k_\Delta \langle ISI^\Delta \rangle \\
 \langle \dot{I} \rangle &= -\mu \langle I \rangle + \beta k \langle SI \rangle + \beta_\Delta k_\Delta \langle ISI^\Delta \rangle \\
 \langle \dot{S}S \rangle &= 2\mu \langle SI \rangle - 2\beta(k-1) \langle SSI \rangle \\
 &\quad - 2\beta_\Delta \frac{k_\Delta}{k} (k-2) \langle IIS^\Delta S \rangle \\
 \langle \dot{S}I \rangle &= \mu \langle II \rangle - \mu \langle SI \rangle + \beta(k-1) \langle SSI \rangle \\
 &\quad - \beta(k-1) \langle ISI \rangle - \beta \langle SI \rangle \\
 &\quad + \beta_\Delta \frac{k_\Delta}{k} (k-2) \langle IIS^\Delta S \rangle - 2\beta_\Delta \frac{k_\Delta}{k} \langle ISI^\Delta \rangle \\
 &\quad - \beta_\Delta \frac{k_\Delta}{k} (k-2) \langle IIS^\Delta I \rangle \\
 \langle \dot{I}I \rangle &= -2\mu \langle II \rangle + 2\beta(k-1) \langle ISI \rangle + 2\beta \langle SI \rangle \\
 &\quad + 4\beta_\Delta \frac{k_\Delta}{k} \langle ISI^\Delta \rangle + 2\beta_\Delta \frac{k_\Delta}{k} (k-2) \langle IIS^\Delta I \rangle
 \end{aligned} \tag{16}$$

Here, we remark a property of the model. Analogously to what happens for the SIS model on networks, where the recovery is a 1-body process, and the infection a 2-body one, here, in both the individual-based and the pair-based exact models of simplicial SIS contagion dynamics, we find terms functions of both m -body and $(m+1)$ -body quantities. For instance, the dynamics of $\langle I \rangle$ (1-body variable) depends on $\langle I \rangle$ itself and on $\langle SI \rangle$ (2-body). Compared the model on networks, however, in the simplicial SIS model a 3-body infection process is also present. Consequently, for both the individual-based and the pair-based exact models, the equations governing the evolution of the m -body quantities are determined by m -body, $(m+1)$ -body, and $(m+2)$ -body quantities. Hence, in the simplicial SIS model, the dynamics of $\langle I \rangle$ (1-body variable) depends not only on $\langle I \rangle$ itself and on $\langle SI \rangle$ (2-body), but also on $\langle ISI^\Delta \rangle$ (3-body).

Similarly to what we have done for Eqs. (5), we now close Eqs. (16) at the level of pairs. To this aim, we use the approximations for the triplet densities $\langle ABC \rangle$

at the pair level given by Eqs. (6), (7), and (9). For what concerns the densities of the 4-node motifs, we rely on the closures introduced in [30] (see Eqs. 15), after re-adapting them to the simplicial case. Accordingly, we consider

$$\begin{aligned} \langle IIS^\Delta S \rangle_0 &= \frac{\langle SI \rangle^2 \langle II \rangle \langle SS \rangle}{\langle S \rangle^2 \langle I \rangle^2} \\ \langle IIS^\Delta S \rangle_1 &= \frac{\langle SI \rangle^3 \langle SS \rangle \langle II \rangle}{\langle S \rangle^3 \langle I \rangle^3} \\ \langle IIS^\Delta S \rangle_2 &= \frac{\langle SS \rangle \langle SI \rangle^4 \langle II \rangle}{\langle S \rangle^4 \langle I \rangle^4} \\ \langle IIS^\Delta I \rangle_0 &= \frac{\langle SI \rangle^3 \langle II \rangle}{\langle S \rangle^2 \langle I \rangle^2} \\ \langle IIS^\Delta I \rangle_1 &= \frac{\langle SI \rangle^3 \langle II \rangle^2}{\langle S \rangle^2 \langle I \rangle^4} \\ \langle IIS^\Delta I \rangle_2 &= \frac{\langle SI \rangle^3 \langle II \rangle^3}{\langle S \rangle^2 \langle I \rangle^6} \end{aligned} \quad (17)$$

where we defined the 4-node motif states densities as a function of the pair state variables. Summing up, Eqs. (16) along with the expressions (6), (7), (9), and (17) constitute a closed approximation for the pair-based mean-field simplicial SIS model.

IV. RESULTS

In this section we analyse the pair-based approximation of the simplicial SIS model, and compare it with the corresponding individual-based approximation. In particular, we will focus on the fraction of infected individuals, denoted as $\rho(t) = \langle I(t) \rangle$, and on its steady-state value ρ^* . We will study ρ^* as a function of the model parameters, specifically the rescaled infection rates $\lambda = k\beta/\mu$ and $\lambda_\Delta = k_\Delta\beta_\Delta/\mu$, and also compare the prediction of the models with the results of numerical, stochastic simulations on a random simplicial complex (RSC) [20]. We will show that pair-based simplicial SIS model better predicts both the epidemics threshold and the nature of the phase transitions, i.e., continuous or discontinuous, of the spreading process.

While for the individual-based model the stationary density ρ^* can be evaluated analytically [20], the pair-based model is not analytically tractable, and we were not able to find a closed-form expression for the steady-state equilibrium. For this reason, the stationary density ρ^* is obtained by numerically integrating Eqs. (16) for a sufficiently long time window, such that the system reaches the steady-state.

Since in the individual-based approximation of the simplicial SIS model, ρ^* as a function of λ can exhibit a bistable regime [20], to check whether the same behavior also appears in the pair-based approximation, for each setting of the parameters we carry out simulations starting from two different initial conditions of $\rho(0)$, one with a very low fraction of initially infected individuals, $\rho(0) = 10^{-6}$, and another with a higher fraction,

$\rho(0) = 0.8$. Once fixed the initial fraction of infected individuals $\langle I \rangle_0$, from which it follows $\langle S \rangle_0 = 1 - \langle I \rangle_0$, the initial conditions of the state variables of the pair-based approximation are set as:

$$\begin{aligned} \langle SS \rangle_0 &= \langle S \rangle_0^2 \\ \langle SI \rangle_0 &= \langle S \rangle_0 \langle I \rangle_0 \\ \langle II \rangle_0 &= \langle I \rangle_0^2 \end{aligned} \quad (18)$$

Finally, to integrate the pair-based approximation, we need to evaluate ϕ , namely the fraction of closed triangles over all triplets in the simplicial complex, which is an input parameter of Eqs. (15). For a RSC with N nodes, an average number of 1-simplices equal to k , and an average number of 2-simplices equal to k_Δ , the expected number of closed triplets is given by:

$$\mathbb{E}(\mathcal{T}) \approx \binom{N}{3} \frac{k}{(N-1)} + \binom{N}{3} \frac{2k_\Delta}{(N-1)(N-2)}. \quad (19)$$

After some algebraic manipulations and using the definition in Eq. (8), the global clustering coefficient ϕ for the RSC can be approximated as

$$\phi \approx \frac{k^2(N-2)}{(N-1)^2(k-1)} + \frac{2k_\Delta}{k(k-1)}. \quad (20)$$

For what concerns the stochastic simulations on the RSC, they are carried out on a RSC with $N = 2000$ nodes, $k \approx 20$ and $k_\Delta \approx 6$, setting $\rho(0)N$ randomly chosen nodes in the infectious state. For each setting of the model parameters, we perform $M = 100$ runs, each one using a different instance of the RSC model, and we evaluate the stationary state ρ^* as the average over the last 100 values of $\rho(t)$. We run the simulations with two different values of $\rho(0)$, namely $\rho(0) = 0.001$ and $\rho(0) = 0.8$.

We start illustrating our results by comparing the stationary density ρ^* obtained from the stochastic simulations, the individual-based, and the pair-based model for different sets of parameters. In particular, Fig. 3(a) shows ρ^* as a function of the rescaled infectivity λ for three different values of λ_Δ . The result of the individual-based model is represented by a dashed black curve, while the result of the pair-based model is represented by a continuous black curve. The values obtained from stochastic simulations on the RSC with $\rho(0) = 0.001$ are depicted as blue dots, and those with an initial density of $\rho(0) = 0.8$ are depicted as yellow dots.

First, we observe that both the individual-based and the pair-based model correctly predict the existence of a region of values of λ for which the system is bistable, and that the transition from the disease-free equilibrium, $\rho^* = 0$, to the endemic equilibrium, $\rho^* > 0$, is discontinuous. However, the pair-based approximation generally better predicts the behavior of the stochastic simulations on the RSC compared to the one provided by the individual-based approximation. In particular, the individual-based model tends to overestimate the stationary fraction of infected individuals, while the pair-based

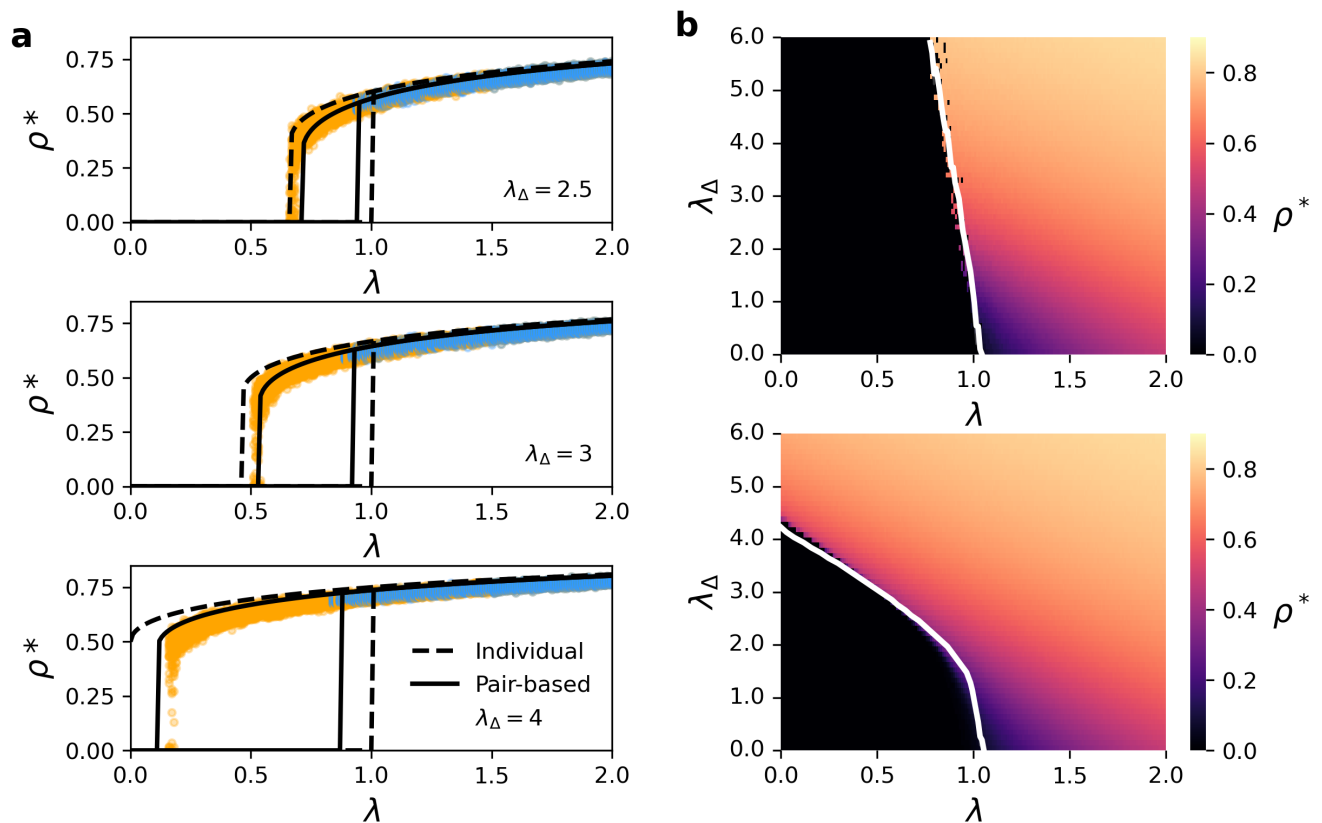


FIG. 3. Steady-state behavior, ρ^* , of the SIS model on a Random Simplicial Complex (RSC) with $N = 2000$, $k = 20$ and $k_\Delta = 6$. (a) Phase diagrams of both individual (black dashed lines) and pair-based (black solid lines) models, compared to the stochastic simulations in three different cases of rescaled infectivities on 2-simplex values λ_Δ . The blue dots represent the values of the stationary densities obtained from $M = 100$ iterations of the stochastic simulations with $\rho(0) = 0.001$, while the orange dots represent the stationary densities obtained with $\rho(0) = 0.8$. (b) The average fractions of steady-state infected individuals obtained by means of stochastic simulations on the RSC in the parameter space $(\lambda, \lambda_\Delta)$. In the upper panel the solid line represent the epidemic threshold values predicted by the Pair-based model, while in the bottom the solid line represent the critical lambda values obtained by the Pair-based model.

model is in better agreement with the numerical simulations. Our analysis also shows that the pair-based approximation better identifies the two epidemic thresholds delimiting the region of bistability, while the individual-based model overestimates the width of this region. The individual-based model, in fact, underestimates the first threshold, which represents the critical point for the simulations started with a high fraction of infected individuals, i.e., $\rho(0) = 0.8$, and, at the same time, overestimates the second threshold, which represents the critical point for the simulations started with a low fraction of infected individuals, i.e. $\rho(0) = 0.001$. Indeed, while the individual-based approximation predicts a transition at $\lambda = 1$ for any value of λ_Δ , the stochastic simulations display a discontinuity at values of $\lambda < 1$ that depends on λ_Δ , a behavior that is well reproduced by the pair-based approximation. We then investigate the behavior of ρ^* as a function of both λ and λ_Δ , comparing the results of the stochastic simulations with the value obtained from the pair-based approximation. Fig. 3(b) shows the results

for $\rho(0) = 0.8$ (upper panel) and $\rho(0) = 0.001$ (lower panel). In both cases, the color represents the value of ρ^* obtained from the stochastic simulations on the RSC, while the white curves represent the critical points derived from the pair-based approximation. Specifically, in the upper panel, where the pair-based model is initiated with a high value for the initial condition $\rho(0)$, the white curve corresponds to the first threshold that delineates the region of bistability and that we here indicate as λ_c . Instead, in the lower panel, obtained starting from the smaller value of the initial condition $\rho(0)$, the white curve corresponds to the second threshold that we denote as λ^* . As shown in Fig. 3(b), both λ_c and λ^* decrease as a function of λ_Δ , meaning that the three-body interactions boost the spreading process by decreasing the thresholds to observe an endemic behavior. In addition, the distinct rates of decrease observed in λ_c and λ^* as a function of λ_Δ suggest that the width of the bistable region increases with the intensity of the three-body interactions. Such a dependence of the thresholds on λ_Δ is well reproduced by

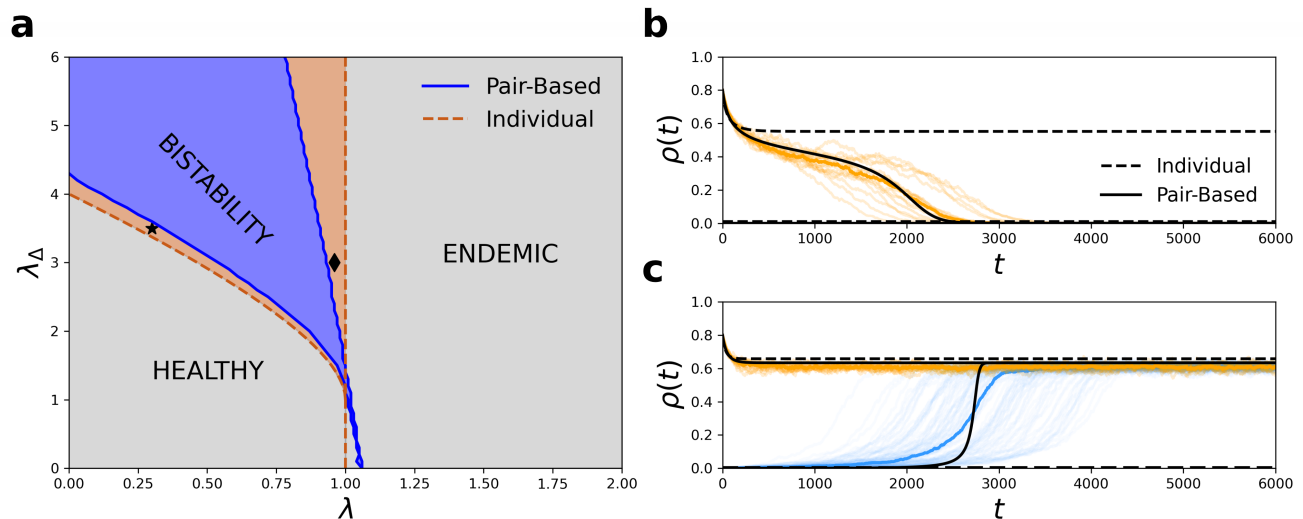


FIG. 4. Region of bistability of the SIS model and temporal evolution of the fraction of infected individuals. (a) Phase diagram, in the parameter space $(\lambda, \lambda_\Delta)$, highlighting the region of bistability obtained from the individual-based approximation (in orange) and the one derived from the pair-based approximation (in blue). (b) Temporal evolution of the fraction of infected individuals $\rho(t)$ for $(\lambda, \lambda_\Delta) = (0.3, 3.5)$, which corresponds to the point marked with a black star in (a), for the individual-based (dashed line) and pair-based (continuous line) approximations. (c) Temporal evolution of the fraction of infected individuals $\rho(t)$ for $(\lambda, \lambda_\Delta) = (0.95, 3)$, which corresponds to the point marked with a black star in (a), for the individual-based (dashed line) and pair-based (continuous line) approximations. In both panels (b) and (c), for each mean-field model we have illustrated the temporal evolution from two distinct initial conditions, namely $\rho(0) = 0.8$ and $\rho(0) = 0.001$. The colored curves depict $M = 100$ realizations of the spreading process on a RSC, with the colors representing the two different initial conditions of the simulations, namely $\rho(0) = 0.8$ (orange) and $\rho(0) = 0.001$ (blue).

the pair-based approximation of the simplicial SIS model.

Next, we compare the region of bistability predicted by the individual-based and pair-based approximations. Fig. 4(a) shows the model behavior as a function of λ and λ_Δ , with the orange area indicating the region of bistability predicted by the individual-based approximation and the blue area that by pair-based approximation. The darker lines represent the thresholds associated to the two approximations. Finally, the gray area represents the region that in both models corresponds to a single equilibrium, either disease-free $\rho^* = 0$ or endemic $\rho^* > 0$. Since the pair-based approximation well predicts the dependence of the critical points on λ_Δ , as shown in Fig. 3(b), then, Fig. 4(a) provides another indication that the individual-based model overestimates the width of the region of bistability, by simultaneously underestimating λ_c and overestimating λ^* . Overall, these results demonstrate that the pair-based approximation of the simplicial SIS process provides a better description of the spreading process on simplicial complexes compared to the individual-based mean-field approximation.

We conclude this section by illustrating in Fig. 4(b)-(c) the time evolution of $\rho(t)$ obtained from stochastic simulations on the RSC and from the individual-based and the pair-based approximations for two settings of $(\lambda, \lambda_\Delta)$, namely $(\lambda, \lambda_\Delta) = (0.3, 3.5)$ and $(\lambda, \lambda_\Delta) = (0.95, 3)$. These values correspond to the points of the phase

agram in Fig. 4(a) marked with a star and a diamond, respectively. In both cases, the individual-based approximation predicts the existence of two stable equilibria, while the pair-based approximation predicts a single one. Specifically, in the pair-based approximation, the steady-state equilibrium corresponds to a disease-free state for $(\lambda, \lambda_\Delta) = (0.3, 3.5)$ and to an endemic state for $(\lambda, \lambda_\Delta) = (0.95, 3)$. As shown in Fig. 4(b)-(c), the time evolution of $\rho(t)$ calculated from the stochastic simulations converges to a single equilibrium point, independently from the system initial conditions, as correctly predicted by the pair-based approximation. The model is also able to reproduce the average behavior of the temporal evolution of the epidemic process.

V. CONCLUSIONS

In this work, we have introduced a pair-based mean-field approximation of the simplicial SIS model. Firstly, we derived the exact equations for the system, emphasizing the distinctions between our approach and the individual-based one. We also introduced suitable closures to obtain a closed form for the model. Then, we compared the behavior of both approximations (the individual-based and the pair-based) and contrasted the results with those obtained from stochastic simulations

on random simplicial complexes. Our results demonstrate that the pair-based approach offers a more accurate approximation of the SIS contagion process when higher-order interactions are present. This is evident in several aspects, including the extent of the region exhibiting bistability, the nature of the transition from a disease-free to an endemic state, and the average time evolution of the fraction of infected individuals.

The pair-based approximation presented in our work

is restricted to cases where higher-order interactions are represented by simplicial complexes. However, it can be extended to the more general scenario of hypergraphs by taking into account that there can be three-body interactions not correlated with two-body interactions. Another possible direction for future work is to include both dynamical correlations and degree heterogeneity, so that to extend the range of the hypernetworks whose behavior can be approximated by these mean-field models.

-
- [1] István Z Kiss, Joel C Miller, Péter L Simon, et al. Mathematics of epidemics on networks. *Cham: Springer*, 598, 2017.
- [2] Romualdo Pastor-Satorras, Claudio Castellano, Piet Van Mieghem, and Alessandro Vespignani. Epidemic processes in complex networks. *Reviews of modern physics*, 87(3):925, 2015.
- [3] Jesus Gómez-Gardenes, L Lotero, SN Taraskin, and FJ Pérez-Reche. Explosive contagion in networks. *Scientific reports*, 6(1):19767, 2016.
- [4] Jae Dong Noh and Heiko Rieger. Random walks on complex networks. *Physical review letters*, 92(11):118701, 2004.
- [5] Jesús Gómez-Gardenes and Vito Latora. Entropy rate of diffusion processes on complex networks. *Physical Review E*, 78(6):065102, 2008.
- [6] Stefano Boccaletti, Vito Latora, Yamir Moreno, Martin Chavez, and D-U Hwang. Complex networks: Structure and dynamics. *Physics reports*, 424(4-5):175–308, 2006.
- [7] Vito Latora, Vincenzo Nicosia, and Giovanni Russo. *Complex networks: principles, methods and applications*. Cambridge University Press, 2017.
- [8] Federico Battiston, Giulia Cencetti, Iacopo Iacopini, Vito Latora, Maxime Lucas, Alice Patania, Jean-Gabriel Young, and Giovanni Petri. Networks beyond pairwise interactions: structure and dynamics. *Physics Reports*, 874:1–92, 2020.
- [9] Claude Berge. *Hypergraphs: combinatorics of finite sets*, volume 45. Elsevier, 1984.
- [10] Ronald H Atkin. From cohomology in physics to q-connectivity in social science. *International journal of man-machine studies*, 4(2):139–167, 1972.
- [11] Timoteo Carletti, Duccio Fanelli, and Sara Nicoletti. Dynamical systems on hypergraphs. *Journal of Physics: Complexity*, 1(3):035006, 2020.
- [12] Timoteo Carletti, Federico Battiston, Giulia Cencetti, and Duccio Fanelli. Random walks on hypergraphs. *Physical review E*, 101(2):022308, 2020.
- [13] Michael T Schaub, Austin R Benson, Paul Horn, Gabor Lippner, and Ali Jadbabaie. Random walks on simplicial complexes and the normalized hodge 1-laplacian. *SIAM Review*, 62(2):353–391, 2020.
- [14] Per Sebastian Skardal and Alex Arenas. Abrupt desynchronization and extensive multistability in globally coupled oscillator simplexes. *Physical review letters*, 122(24):248301, 2019.
- [15] Maxime Lucas, Giulia Cencetti, and Federico Battiston. Multiorder laplacian for synchronization in higher-order networks. *Physical Review Research*, 2(3):033410, 2020.
- [16] Lucia Valentina Gambuzza, Francesca Di Patti, Luca Gallo, Stefano Lepri, Miguel Romance, Regino Criado, Mattia Frasca, Vito Latora, and Stefano Boccaletti. Stability of synchronization in simplicial complexes. *Nature communications*, 12(1):1255, 2021.
- [17] Unai Alvarez-Rodríguez, Federico Battiston, Guilherme Ferraz de Arruda, Yamir Moreno, Matjaž Perc, and Vito Latora. Evolutionary dynamics of higher-order interactions in social networks. *Nature Human Behaviour*, 5(5):586–595, 2021.
- [18] Damon Centola and Michael Macy. Complex contagions and the weakness of long ties. *American journal of Sociology*, 113(3):702–734, 2007.
- [19] Guilherme Ferraz de Arruda, Giovanni Petri, and Yamir Moreno. Social contagion models on hypergraphs. *Physical Review Research*, 2(2):023032, 2020.
- [20] Iacopo Iacopini, Giovanni Petri, Alain Barrat, and Vito Latora. Simplicial models of social contagion. *Nature communications*, 10(1):1–9, 2019.
- [21] Federico Malizia, Santiago Lamata-Otín, Mattia Frasca, Vito Latora, and Jesús Gómez-Gardeñes. Hyperedge overlap drives explosive collective behaviors in systems with higher-order interactions. *arXiv preprint arXiv:2307.03519*, 2023.
- [22] Matthew J Keeling. The effects of local spatial structure on epidemiological invasions. *Proceedings of the Royal Society of London. Series B: Biological Sciences*, 266(1421):859–867, 1999.
- [23] Kieran J Sharkey, Istvan Z Kiss, Robert R Wilkinson, and Peter L Simon. Exact equations for sir epidemics on tree graphs. *Bulletin of mathematical biology*, 77:614–645, 2015.
- [24] Mattia Frasca and Kieran J Sharkey. Discrete-time moment closure models for epidemic spreading in populations of interacting individuals. *Journal of theoretical biology*, 399:13–21, 2016.
- [25] Federico Malizia, Luca Gallo, Mattia Frasca, Vito Latora, and Giovanni Russo. Individual-and pair-based models of epidemic spreading: Master equations and analysis of their forecasting capabilities. *Physical Review Research*, 4(2):023145, 2022.
- [26] Joan T Matamalas, Sergio Gómez, and Alex Arenas. Abrupt phase transition of epidemic spreading in simplicial complexes. *Physical Review Research*, 2(1):012049, 2020.
- [27] Giulio Burgio, Sergio Gómez, and Alex Arenas. Triadic approximation for contagions on higher-order networks. *arXiv preprint arXiv:2306.11441*, 2023.
- [28] John G Kirkwood. Statistical mechanics of fluid mixtures. *The Journal of chemical physics*, 3(5):300–313, 1935.

[29] The formula can be understood as follows:
 $P(AB \cap BC \cap CA) = P(AB \cap BC|CA)P(CA)$. Now
 $P(AB \cap BC|CA) = P(AB|BC \cap CA) \cdot P(BC|CA)$.
 We can write $P(AB|BC \cap CA) = \frac{P(AB)}{P(A)P(B)}$, and use
 the approximation $P(AB|BC \cap CA) = \frac{P(AB)}{P(A)P(B)}$.

Substituting in the previous expression one has
 $P(AB \cap BC|CA) = \frac{P(AB)}{P(A)P(B)} \cdot \frac{P(BC)}{P(C)}$
 from which it follows $P(AB \cap BC \cap CA) =$
 $P(AB)P(BC)P(CA)/(P(A)P(B)P(C))$.
 [30] Thomas House, Geoffrey Davies, Leon Danon, and
 Matt J Keeling. A motif-based approach to network epi-
 demics. Bulletin of Mathematical Biology, 71(7):1693–
 1706, 2009.